
FEDERATED DOMAIN ADAPTATION VIA GRADIENT PROJECTION

Enyi Jiang*
enyij2@illinois.edu
UIUC

Yibo Jacky Zhang*
yiboz@stanford.edu
Stanford

Oluwasanmi Koyejo
sanmi@stanford.edu
Stanford

ABSTRACT

Federated Domain Adaptation (FDA) describes the federated learning setting where a set of source clients work collaboratively to improve the performance of a target client and where the target client has limited labeled data. The domain shift between the source and target domains, combined with limited samples in the target domain, makes FDA a challenging problem, e.g., common techniques such as FedAvg and fine-tuning fail with a large domain shift. To fill this gap, we propose Federated Gradient Projection (FedGP), a novel aggregation rule for FDA, used to aggregate the source gradients and target gradient during training. Further, we introduce metrics that characterize the FDA setting and propose a theoretical framework for analyzing the performance of aggregation rules, which may be of independent interest. Using this framework, we theoretically characterize how, when, and why FedGP works compared to baselines. Our theory suggests certain practical rules that are predictive of practice. Experiments on synthetic and real-world datasets verify the theoretical insights and illustrate the effectiveness of the proposed method in practice.

1 Introduction

Federated learning (FL) is a distributed machine learning paradigm that aggregates clients' models on the server without exposing sensitive data (McMahan et al., 2017). In real-world settings such as cell phones or hospitals, one may encounter data heterogeneity and limited labeled data issues across clients. While there are many recent works that focus on minimizing the negative impact of distribution shifts between clients (Wang et al., 2019; Karimireddy et al., 2020; Xie et al., 2020b), yet most of them assume all clients' data are fully labeled. However, in the real world, one often encounters settings where the labels are scarce on some of the clients. To this end, Federated Domain Adaptation (FDA) (Peng et al., 2020; Feng et al., 2021; Wu & Gong, 2021) has been proposed to tackle the problem of how source clients with abundant labeled data can collaborate to boost the performance of a target client. However, current works mainly focus on the unsupervised setting, i.e., assuming the data are all unlabeled on the target client. To our knowledge, we are the first to consider the common setting of limited labeled target data. Specifically, we find that, perhaps surprisingly, noisy gradients computed using limited labeled data can nevertheless provide a useful signal.

To fill the gap, this work considers an FDA setting where a small set of labeled data are available on the target client. We propose a filtering-based gradient projection method FedGP, which extracts and aggregates useful components of the source gradients with the assistance of the target gradient. As illustrated in Figure 1a, FedGP computes a convex combination of the target gradient and its positive projection to the directions of source gradients. We find the projection operation before the convex combination is important. As illustrated in Figure 1b, experimentally, a convex combination of the source and target gradients (FedDA) is ineffective. Our empirical observations highlight the conceptual and theoretical gap. This motivates the following questions, which we seek to answer rigorously.

How, when, and why does FedGP work better than other baselines?

*Equal contribution

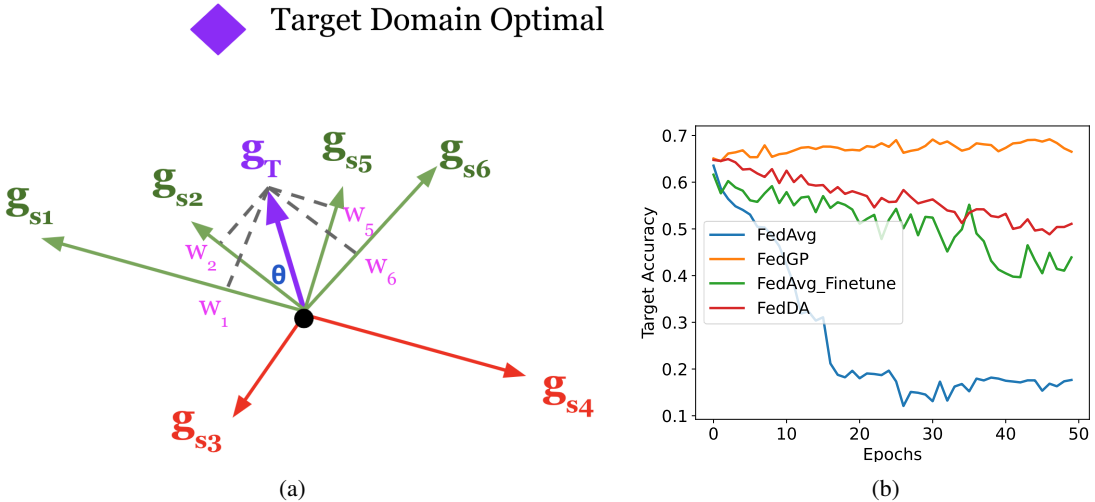


Figure 1: (a) FedGP filters out the negative source gradients g_s (colored in red) and then convexly combines the target gradient g_T and its projections to the directions of the remaining source gradients (green ones). (b) FedAvg, FedDA, and fine-tuning fail to work when target and source distributions are largely different (Fashion-MNIST with a 0.6 noise level on the target distribution) with diverged behaviors. Further details are in the experiments.

To the best of our knowledge, there are no theoretical foundations for the FDA problem that systematically analyze the behaviors of different aggregation rules. Thus, to answer our theoretical questions, we propose a first theoretical framework that formally defines two metrics to characterize specific FDA settings and uses these metrics to explain the performance of FDA aggregation rules. The two metrics characterize (i) the difference between source and target domains, and (ii) the scarcity of the training data in the target domain. Using the resulting framework, potentially of broader interest, we theoretically analyze the behavior of FedGP and provide answers to the theoretical question. The conclusions from the theory coincide with our empirical observations.

Summary of Contributions.

- We propose FedGP to effectively address FDA with the large shifts and limited labeled target data.
- We propose a theoretical framework for analyzing the performance of FDA aggregation rules, which may be of broader interest. Within this framework, we theoretically answer the question of “*how, when, and why does FedGP work better than other baselines?*”
- We empirically analyze the behavior of various aggregation rules with varying extents of distribution shifts between source and target clients, showing that our theory is predictive of practice. We validate the effectiveness of FedGP on real-world datasets.

2 Related Work

Data heterogeneity and label deficiency in federated learning. Distribution shifts between clients remain a crucial challenge in FL. Current work often focuses on improving the aggregation rules: Karimireddy et al. (2020) uses control variates and Xie et al. (2020b) clusters the client weights via EM algorithm to correct the drifts among clients. While existing work often assumes that local training is fully supervised for all clients, label deficiency problems may affect many clients. Recent works have addressed the label deficiency problem with self-supervision or semi-supervision for personalized models (Jeong et al., 2020; He et al., 2021; Yang et al., 2021). Compared to this work, we explore a new setting with fully-labeled source clients and one target client with limited labels.

Federated domain adaptation. There is a considerable amount of recent work on multi-source domain adaptation in the unsupervised setting, with recent highlights in adversarial training (Saito et al., 2018; Zhao et al., 2018), knowledge distillation (Nguyen et al., 2021), and source-free methods (Liang et al., 2020). Peng et al. (2020); Li et al. (2020) is the first to extend MSDA into an FL setting; they apply adversarial adaptation techniques to align the representations of nodes. More recently, in KD3A (Feng et al., 2021) and COPA (Wu & Gong, 2021), the server with unlabeled target samples aggregates the local models by learning the importance of each source domain via knowledge distillation and collaborative optimization. However, training with unlabeled data every round is

computationally expensive, and the signals coming from the unlabeled data are noisy and sometimes misleading. In contrast to prior work for the unsupervised setting, our framework assumes a small number of labeled samples available on the target client and provides the theoretical analysis of different aggregation rules using the proposed theoretical framework.

Using additional gradient information in FL. Model updates in each communication round may provide valuable insights into client convergence directions. This idea has been explored for robustness in FL, particularly with untrusted clients. For example, Zeno++ (Xie et al., 2020a) and FiTrust (Cao et al., 2021) leverage the additional gradient computed from a small clean training dataset on the server to compute the scores of candidate gradients for detecting the malicious adversaries. In contrast, our work uses the additional gradient signal from the labeled target samples for the FDA problem. We propose a new aggregation method FedGP to boost FDA performances with a filtering-based gradient projection.

3 The Gradient Projection Aggregation Method

In this section, we introduce the problem of Federated Domain Adaptation and then define the gradient projection aggregation rule.

Notation. Let \mathcal{D} be a data domain² on a ground set \mathcal{Z} . In our supervised setting, a data point $z \in \mathcal{Z}$ is the tuple of input and output data³. We denote the loss function as $\ell : \Theta \times \mathcal{Z} \rightarrow \mathbb{R}$ where the parameter space is $\Theta = \mathbb{R}^m$; an m -dimensional Euclidean space. The population loss is $\ell_{\mathcal{D}}(\theta) := \mathbb{E}_{z \sim \mathcal{D}} \ell(\theta, z)$, where $\mathbb{E}_{z \sim \mathcal{D}}$ is the expectation w.r.t. \mathcal{D} . Let $\widehat{\mathcal{D}}$ be a finite sample dataset drawn from \mathcal{D} , then $\ell_{\widehat{\mathcal{D}}}(\theta) := \frac{1}{|\widehat{\mathcal{D}}|} \sum_{z \in \widehat{\mathcal{D}}} \ell(\theta, z)$, where $|\widehat{\mathcal{D}}|$ is the size of the dataset. We use $[N] := \{1, 2, \dots, N\}$. By default, $\langle \cdot, \cdot \rangle$ and $\|\cdot\|$ respectively denote the Euclidean inner product and Euclidean norm.

In FDA, there are N source clients with their respective source domains $\{\mathcal{D}_{S_i}\}_{i \in [N]}$ and a target client with the target domain \mathcal{D}_T . For $\forall i \in [N]$, the i^{th} source client holds a dataset $\widehat{\mathcal{D}}_{S_i}$ and the target client holds a dataset $\widehat{\mathcal{D}}_T$. We consider the case that $|\widehat{\mathcal{D}}_T|$ is relatively small.

All source clients collaborate in a federated manner to improve the global model for the target domain, i.e., we aim to find a model parameter θ such that the population loss function of the target domain $\ell_{\mathcal{D}_T}(\theta)$ is minimized. This is done by iteratively updating the global model parameter θ with gradients from the source clients and the gradient from the target clients, i.e.,

$$\theta \leftarrow \theta - \mu \cdot \text{Aggr}(\{\nabla \ell_{\widehat{\mathcal{D}}_{S_i}}(\theta)\}_{i \in [n]}, \nabla \ell_{\widehat{\mathcal{D}}_T}(\theta)),$$

where $\nabla \ell$ is the gradient, μ is the step size and Aggr is an operation that aggregates the gradients, e.g., FedAvg.

The choice of aggregation is vital. As illustrated in Figure 1, FedAvg, i.e., simply taking the average of all gradients can lead to undesirable results due to the source-target domain shift. This highlights a need for a better aggregation approach.

To achieve this, we propose the FedGP aggregation.

Definition 3.1 (FedGP). Let $g_i := \nabla \ell_{\widehat{\mathcal{D}}_{S_i}}(\theta)$ and $g_T = \nabla \ell_{\widehat{\mathcal{D}}_T}(\theta)$, and let $\beta \in [0, 1]$ be a parameter that balances between the source and target domain. $\text{FedGP}(\{g_i\}_{i=1}^N, g_T; \beta)$ is computed as

$$(1 - \beta)g_T + \frac{\beta}{N} \sum_{i=1}^N \text{Proj}_+(g_T | g_i),$$

where $\text{Proj}_+(g_T | g_i) = \max\{\langle g_T, g_i \rangle, 0\} g_i / \|g_i\|^2$ is the operation that projects g_T to the positive direction of g_i .

We also consider Federated Domain Adaptation, i.e., FedDA, a baseline that shares the same intuition of combining and balancing both the source and target gradients, but skips the projection, defined:

Definition 3.2 (FedDA). Denote $g_i := \nabla \ell_{\widehat{\mathcal{D}}_{S_i}}(\theta)$ and $g_T = \nabla \ell_{\widehat{\mathcal{D}}_T}(\theta)$, and let $\beta \in [0, 1]$ be a parameter that balances between the source and target domain.

$$\text{FedDA}(\{g_i\}_{i=1}^N, g_T; \beta) = (1 - \beta)g_T + \frac{\beta}{N} \sum_{i=1}^N g_i.$$

²In this paper, the terms distribution and domain are used interchangeably.

³Let x be the inputs and y be the targets, then $z = (x, y)$. We do not need the function details for our analysis, so will not use it.

4 Theoretical Analysis

We introduce a general framework for analyzing aggregation rules, then use this to analyze FedGP in comparison to three baselines, i.e., FedDA, target gradient only, source gradients only. The analysis shows conditions under which FedGP is better than alternatives. All proofs are deferred to section A in the appendix.

Additional Notation. We use additional notation to motivate a functional view of FDA. Let $g_{\mathcal{D}} : \Theta \rightarrow \Theta$ with $g_{\mathcal{D}}(\theta) := \nabla \ell_{\mathcal{D}}(\theta)$. Given a distribution π on the parameter space Θ , we define an inner product $\langle g_{\mathcal{D}}, g_{\mathcal{D}'} \rangle_{\pi} = \mathbb{E}_{\theta \sim \pi}[\langle g_{\mathcal{D}}(\theta), g_{\mathcal{D}'}(\theta) \rangle]$. The inner product induces the L^{π} -norm on $g_{\mathcal{D}}$ as $\|g_{\mathcal{D}}\|_{\pi} := \sqrt{\mathbb{E}_{\theta \sim \pi} \|g_{\mathcal{D}}(\theta)\|^2}$. Given an aggregation rule $\text{Aggr}(\cdot)$, we denote $\widehat{g}_{\text{Aggr}}(\theta) = \text{Aggr}(\{g_{\mathcal{D}_{S_i}}(\theta)\}_{i=1}^N, g_{\widehat{\mathcal{D}}_T}(\theta))$.

4.1 A general framework for analyzing FDA

Our framework for analyzing FDA will ask, for a random parameter sampled from π , a distribution of updates over training, how much does a certain aggregation improve the performance of one step of gradient descent? This is crucial information, as it characterizes the convergence quality for each aggregation rule. To analyze an aggregation rule, it is further necessary to characterize the specific FDA setting. For example, the behavior of an aggregation rule varies with the degree and nature of source-target domain shift, and labeled sample size in the target domain. We propose the following metric to quantify the source-domain shift. Let \mathcal{D}_S be the average of each source domain distribution \mathcal{D}_{S_i} (more formally, the average of their corresponding probability measures). Thus, we can define a source-target domain distance as the L^{π} -norm of the difference between the source and target gradient functions.

Definition 4.1 (L^{π} Source-Target Domain Distance).

$$d_{\pi}(\mathcal{D}_S, \mathcal{D}_T) := \|g_{\mathcal{D}_T} - g_{\mathcal{D}_S}\|_{\pi} = \|g_{\mathcal{D}_T} - \frac{1}{N} \sum_{i=1}^N g_{\mathcal{D}_{S_i}}\|_{\pi}.$$

This proposed metric d_{π} has some properties inherited from being a distance, including: (i. *symmetry*) $d_{\pi}(\mathcal{D}_S, \mathcal{D}_T) = d_{\pi}(\mathcal{D}_T, \mathcal{D}_S)$; (ii. *triangle inequality*) Given any data distribution \mathcal{D}' we have $d_{\pi}(\mathcal{D}_S, \mathcal{D}_T) \leq d_{\pi}(\mathcal{D}_S, \mathcal{D}') + d_{\pi}(\mathcal{D}_T, \mathcal{D}')$; (iii. *zero property*) For any data distribution \mathcal{D} : $d_{\pi}(\mathcal{D}, \mathcal{D}) = 0$.

To formalize the effect of target domain sample size, we assume that each sample in $\widehat{\mathcal{D}}_T$ is sampled i.i.d. from \mathcal{D}_T . Thus, the distance between $\widehat{\mathcal{D}}_T$ and \mathcal{D}_T defines the effect of limited data, as a target domain variance.

Definition 4.2 (L^{π} Target Domain Variance).

$$\sigma_{\pi}^2(\widehat{\mathcal{D}}_T) := \mathbb{E}_{\widehat{\mathcal{D}}_T} \|g_{\mathcal{D}_T} - g_{\widehat{\mathcal{D}}_T}\|_{\pi}^2,$$

where $\mathbb{E}_{\widehat{\mathcal{D}}_T}$ denotes taking expectation over random fixed-size dataset $\widehat{\mathcal{D}}_T$ where each of the data points are sampled i.i.d. from \mathcal{D}_T .

Since we assume target data samples are i.i.d., we can see that $\widehat{\mathcal{D}}_T \rightarrow \mathcal{D}_T$ with increasing sample size, resulting in a corresponding decrease in $\sigma_{\pi}^2(\mathcal{D}_T)$.

Note that we don't consider the source domain variance – since we are primarily focused on the generalization performance on the target domain, we can simply let \mathcal{D}_{S_i} be the empirical distribution of the source dataset(s). Moreover, for FDA, one expects the sample variance of $\widehat{\mathcal{D}}_{S_i}$ to be small – with abundant source data – compared to the variance of the target domain.

Next, we define an aggregation error term that will be useful for our analysis.

Definition 4.3 (L^{π} Error of an aggregation rule $\text{Aggr}(\cdot)$).

$$\Delta_{\text{Aggr}}^2 := \mathbb{E}_{\widehat{\mathcal{D}}_T} \|g_{\mathcal{D}_T} - \widehat{g}_{\text{Aggr}}\|_{\pi}^2.$$

Note on notation. We will sometimes the term *Delta error* to refer to Δ_{Aggr}^2 . With this background, we can now state a theorem that bounds the aggregation rule error.

Theorem 4.4. Consider model parameter $\theta \sim \pi$ and an aggregation rule $\text{Aggr}(\cdot)$ with step size $\mu > 0$. Define the updated parameter as

$$\theta^+ := \theta - \mu \widehat{g}_{\text{Aggr}}(\theta).$$

Assuming the gradient $\nabla \ell(\theta, z)$ is γ -Lipschitz in θ for any z , and let the step size $\mu = \frac{1}{\gamma}$, we have

$$\mathbb{E}_{\widehat{\mathcal{D}}_T, \theta} [\ell_{\mathcal{D}_T}(\theta^+) - \ell_{\mathcal{D}_T}(\theta)] \leq -\frac{1}{2\gamma} (\|g_{\mathcal{D}_T}\|_{\pi}^2 - \Delta_{\text{Aggr}}^2).$$

As we can see, $\Delta_{\text{Aggr}}^2 < \|g_{\mathcal{D}_T}\|_\pi^2$ implies that the model parameter after the update is better on the target domain \mathcal{D}_T in expectation. Therefore, one expects an aggregation rule with a small L^π -error to perform better as measured by the population target domain loss function $\ell_{g_{\mathcal{D}_T}}$. Charmingly, the L^π -error shares a similar structure as the L^π source-target distance $d_\pi(\mathcal{D}_S, \mathcal{D}_T)$ and the L^π target domain variance $\sigma_\pi^2(\widehat{\mathcal{D}}_T)$.

Error analysis for simple cases. The L^π -error of two of the baseline aggregation rules, i.e., target gradient only, and averaged source gradients only, are straightforward. By definition, we have that

$$\begin{aligned}\Delta_{\text{target only}}^2 &= \sigma_\pi^2(\widehat{\mathcal{D}}_T) \\ \Delta_{\text{source only}}^2 &= d_\pi^2(\mathcal{D}_S, \mathcal{D}_T).\end{aligned}$$

This immediate result demonstrates the usefulness of the proposed framework.

More intuition for good aggregation rules thus emerges: if $\widehat{g}_{\text{Aggr}}$ only uses the target gradient then the error is the target domain variance; if $\widehat{g}_{\text{Aggr}}$ only uses the source gradients then the error is the source-target domain bias. Therefore, a good aggregation method must strike a balance between the bias and variance, i.e., a bias-variance trade-off.

4.2 Analysis of FedGP and FedDA

Both the FedGP and FedDA combine the source and target gradients and find a different operating point of the bias-variance trade-off. How might they compare to each other, and which method is the best under what conditions? We answer this question next.

We first present the result for FedDA, and then move to the more complex FedGP.

Theorem 4.5. *Consider FedDA (Definition 3.2). We have*

$$\Delta_{\text{FedDA}}^2 = (1 - \beta)^2 \sigma_\pi^2(\widehat{\mathcal{D}}_T) + \beta^2 d_\pi^2(\mathcal{D}_S, \mathcal{D}_T).$$

From the theorem, we can see the benefits of combining the source and target domain gradients: with a proper choice of β , Δ_{FedDA}^2 can be smaller than $\sigma_\pi^2(\widehat{\mathcal{D}}_T)$ and $d_\pi^2(\mathcal{D}_S, \mathcal{D}_T)$.

Unlike FedDA, FedGP combines the gradients in a non-linear way which complicates the analysis. For simplicity, we analyze the case where there is only one source client.

Theorem 4.6. *Consider FedGP (Definition 3.1) in the setting where there is only one source client. We have*

$$\begin{aligned}\Delta_{\text{FedGP}}^2 &= (1 - \beta)^2 \sigma_\pi^2(\widehat{\mathcal{D}}_T) + \beta^2 E_{\theta, \widehat{\mathcal{D}}_T} [\widehat{\delta}(\theta) \tau^2(\theta) \|g_{\mathcal{D}_T}(\theta) - g_{\mathcal{D}_S}(\theta)\|^2] \\ &+ (2\beta - \beta^2) \mathbb{E}_{\theta, \widehat{\mathcal{D}}_T} \widehat{\delta}(\theta) \langle g_{\widehat{\mathcal{D}}_T}(\theta) - g_{\mathcal{D}_T}(\theta), u_{\mathcal{D}_S}(\theta) \rangle^2 + \\ &+ 2\beta(1 - \beta) \mathbb{E}_{\theta, \widehat{\mathcal{D}}_T} [\widehat{\delta}(\theta) \langle g_{\mathcal{D}_T}(\theta), g_{\mathcal{D}_S}(\theta) \rangle \cdot \langle g_{\widehat{\mathcal{D}}_T}(\theta) - g_{\mathcal{D}_T}(\theta), u_{\mathcal{D}_S}(\theta) \rangle] + \beta^2 \mathbb{E}_{\theta, \widehat{\mathcal{D}}_T} [(1 - \widehat{\delta}(\theta)) \|g_{\mathcal{D}_T}(\theta)\|^2].\end{aligned}$$

In the above equation, $\widehat{\delta}(\theta) := \mathbf{1}(\langle g_{\widehat{\mathcal{D}}_T}(\theta), g_{\mathcal{D}_S}(\theta) \rangle > 0)$ is the indicator function and it is 1 if the condition is satisfied. $\tau(\theta) := \frac{\|g_{\mathcal{D}_T}(\theta) \sin \rho(\theta)\|}{\|g_{\mathcal{D}_S}(\theta) - g_{\mathcal{D}_T}(\theta)\|}$ where $\rho(\theta)$ is the angle between $g_{\mathcal{D}_S}(\theta)$ and $g_{\mathcal{D}_T}(\theta)$. Moreover, $u_{\mathcal{D}_S}(\theta) := g_{\mathcal{D}_S}(\theta) / \|g_{\mathcal{D}_S}(\theta)\|$.

For a better intuition of the above theorem, we consider a simple approximation, fixing $\widehat{\delta}(\theta) = \bar{\delta}$ and $\tau(\theta) = \bar{\tau}$, i.e., their expectations⁴. This results in the following.

$$\begin{aligned}\Delta_{\text{FedGP}}^2 &\approx (1 - \beta)^2 \sigma_\pi^2(\widehat{\mathcal{D}}_T) + \beta^2 \bar{\delta} \bar{\tau}^2 d_\pi^2(\mathcal{D}_S, \mathcal{D}_T)^2 \\ &+ (2\beta - \beta^2) \bar{\delta} \mathbb{E}_{\theta, \widehat{\mathcal{D}}_T} \langle g_{\widehat{\mathcal{D}}_T}(\theta) - g_{\mathcal{D}_T}(\theta), u_{\mathcal{D}_S}(\theta) \rangle^2 + \beta^2 (1 - \bar{\delta}) \|g_{\mathcal{D}_T}\|_\pi^2.\end{aligned}$$

The term $\mathbb{E}_{\widehat{\mathcal{D}}_T} \langle g_{\widehat{\mathcal{D}}_T}(\theta) - g_{\mathcal{D}_T}(\theta), u_{\mathcal{D}_S}(\theta) \rangle^2$ is the variance of $g_{\widehat{\mathcal{D}}_T}(\theta)$ when projected to a direction $u_{\mathcal{D}_S}(\theta)$.

We consider a further approximation based on the following intuition: consider a zero-mean random vector $\hat{v} \in \mathbb{R}^m$ with i.i.d. entries \hat{v}_j for $j \in [m]$. After projecting the random vector to a fixed unit vector $u \in \mathbb{R}^m$, the projected variance is $\mathbb{E}\langle \hat{v}, u \rangle^2 = \mathbb{E}(\sum_{j=1}^m \hat{v}_j u_j)^2 = \sum_{j=1}^m \mathbb{E}[\hat{v}_j^2] u_j^2 = \sum_{j=1}^m \frac{\sigma^2(\hat{v})}{m} u_j^2 = \sigma^2(\hat{v})/m$, i.e., the variance becomes much smaller. Therefore, knowing that the parameter space Θ is m -dimensional, combined with the approximation that $g_{\widehat{\mathcal{D}}_T}(\theta) - g_{\mathcal{D}_T}(\theta)$ is element-wise i.i.d., we derive a simpler (approximate) result.

$$\Delta_{\text{FedGP}}^2 \approx \left((1 - \beta)^2 + \frac{(2\beta - \beta^2)\bar{\delta}}{m} \right) \sigma_\pi^2(\widehat{\mathcal{D}}_T) + \beta^2 \bar{\delta} \bar{\tau}^2 d_\pi^2(\mathcal{D}_S, \mathcal{D}_T)^2 + \beta^2 (1 - \bar{\delta}) \|g_{\mathcal{D}_T}\|_\pi^2.$$

⁴This approximation is analogous to a mean-field approximation, where one ignores cross-terms in the expectation of a product.

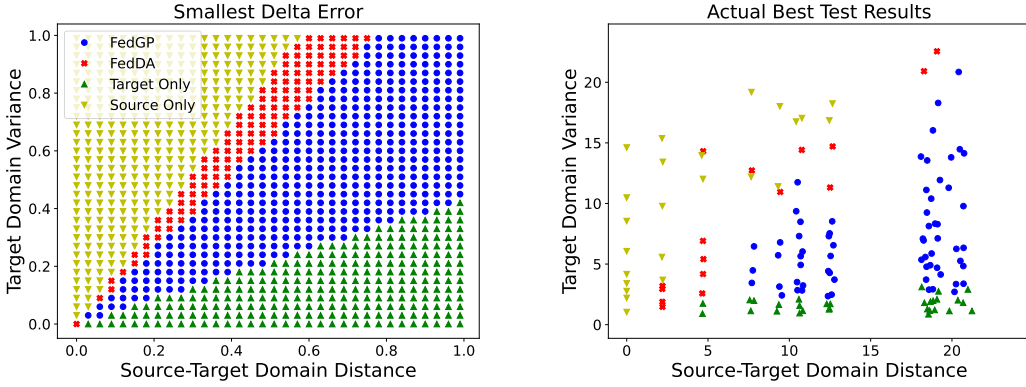


Figure 2: Given specific source-target domain distance $d_\pi(\mathcal{D}_S, \mathcal{D}_T)$ and target domain variance $\sigma_\pi(\hat{\mathcal{D}}_T)$: the **left fig.** shows which aggregation method has the smallest Δ_π^2 error; the **right fig.** shows which aggregation method actually achieves the best test result in the synthetic experiments. The results coincide with what the theory predicts.

4.3 When is FedGP the best?

Comparing FedGP and FedDA. Recall $\Delta_{\text{FedDA}}^2 = (1 - \beta)^2 \sigma_\pi^2(\hat{\mathcal{D}}_T) + \beta^2 d_\pi(\mathcal{D}_S, \mathcal{D}_T)^2$. Noting that $\bar{\delta}, \bar{\tau} \leq 1$, we can draw clear conclusions about the comparison between Δ_{FedGP}^2 and Δ_{FedDA}^2 . When the domain shift is large such that $d_\pi(\mathcal{D}_S, \mathcal{D}_T) \geq \|g_{\mathcal{D}_T}\|_\pi$, with the same β FedGP tolerates more source-target distribution shift than FedDA. Moreover, we argue that FedGP is generally better than FedDA if the dimension m of the parameter space is high, which is true for most real-world applications.

We may compare the four aggregation methods we have analyzed so far, i.e.,

$$\begin{aligned}\Delta_{\text{target only}}^2 &= \sigma_\pi^2(\hat{\mathcal{D}}_T) \\ \Delta_{\text{source only}}^2 &= d_\pi^2(\mathcal{D}_S, \mathcal{D}_T) \\ \Delta_{\text{FedDA}}^2 &= (1 - \beta)^2 \sigma_\pi^2(\hat{\mathcal{D}}_T) + \beta^2 d_\pi(\mathcal{D}_S, \mathcal{D}_T)^2 \\ \Delta_{\text{FedGP}}^2 &\approx \left((1 - \beta)^2 + \frac{(2\beta - \beta^2)\bar{\delta}}{m} \right) \sigma_\pi^2(\hat{\mathcal{D}}_T) + \beta^2 \bar{\delta} \bar{\tau}^2 d_\pi(\mathcal{D}_S, \mathcal{D}_T)^2 + \beta^2 (1 - \bar{\delta}) \|g_{\mathcal{D}_T}\|_\pi^2\end{aligned}$$

Each of the error terms relies on the target domain variance $\sigma_\pi^2(\hat{\mathcal{D}}_T)$, the source-target domain difference $d_\pi^2(\mathcal{D}_S, \mathcal{D}_T)$, and the choice of β . We illustrate this relationship in Figure 2 (left fig.) identifying that which aggregation has the smallest Δ_π^2 error when $\beta = 0.5, \bar{\delta} = 1, \bar{\tau}^2 = 0.5, m = 10$. We note that the choice of $\bar{\delta} = 1$ corresponds to doing FedGP without filtering. As we will show in the experiments, FedGP will become slightly worse if without filtering. We also note that different choices of these hyperparameters do not change the qualitative results of the figure, but may change the transition points.

As we can see from Figure 2 (left fig.), among the four strategies, FedGP is the more robust to big source-target domain shift. We argue that this setting corresponds to most of the FDA problems we care about: (1) the source-target domain shift is big enough such that only using source gradients is not enough; (2) the data on the target client is scarce such that only using the target gradient is not enough. This corresponds to the upper right corner in Figure 2 (left fig.) where FedGP is the best.

Key observations from our theory. We summarize the key observations from our theoretical analysis and Figure 2.

- FedGP is more robust to source-target domain shift than baselines. FedGP is also more robust to limited target domain data when the target domain variance is less than the source-target domain shift.
- (Axis-aligned behavior) Fixing the target dataset and considering the source domain with increasing source-target domain shift (or, equivalently, fixing the target domain and considering source datasets with increasing source-target domain shift). We expect to see that the best method changes from source gradients only, FedDA, FedGP, and finally to target gradients only.

As we will show, these observations are verified by our experiments in the following two sections.

5 Synthetic Data Experiments

The synthetic data experiment aims to bridge the gap between theory and practice by verifying our theoretical insights. Specifically, we generate various source and target datasets and compute the corresponding source-target domain distance $d_\pi(\mathcal{D}_S, \mathcal{D}_T)$ and target domain variance $\sigma_\pi(\widehat{\mathcal{D}}_T)$. We aim to verify if the key observations found by analyzing the Delta error Δ_π^2 still hold for the test performance on the target domain.

In this experiment, we use one-hidden-layer neural networks with sigmoid activation. We generate 9 datasets D_1, \dots, D_9 each consisting of 5000 data points as the following. We first generate 5000 samples $x \in \mathbb{R}^{50}$ from a mixture of 10 Gaussians. The ground truth target is set to be the sum of 100 radial basis functions, the target has 10 samples. We control the randomness and deviation of the basis function to generate datasets with domain shift. As a result, D_2 to D_9 they have increasing domain-shift compared to D_1 . We take D_1 as the target domain. We subsample (uniformly) 9 datasets $\widehat{D}_1^1, \dots, \widehat{D}_1^9$ from D_1 with decreasing number of subsamples. As a result, \widehat{D}_1^1 has the smallest target domain variance, and \widehat{D}_1^9 has the largest.

Methods. For each pair of (D_i, \widehat{D}_1^j) where $i, j = 1, \dots, 9$ from the 81 pairs of datasets. We compute the source-target domain distance $d_\pi(D_i, \widehat{D}_1^j)$ and target domain variance $\sigma_\pi(\widehat{D}_1^j)$ with π being only the initialization parameter. We then train the 2-layer neural network with different aggregation strategies ($\beta = 0.5$ for FedGP and FedDA) with (D_i, \widehat{D}_1^j) and identify which method works the best given the pair of datasets.

Results. As shown in Figure 2 (right fig.), the result largely coincides with what the theory predicts, illustrating that the Delta error is predictive of the actual test performance.

6 Experimental Evaluations

Implementation of FedGP. To implement fine-grained projection for the real model architecture, we compute the cosine similarity between one source client gradient g_i and the target gradient g_T for *each layer* of the model with a threshold of 0. In addition, we align the magnitude of the gradients according to the number of target/source samples, batch sizes, local updates, and learning rates (more details are in Appendix B.2). In this way, we implement FedGP by projecting the target gradient towards source directions.

6.1 Semi-Synthetic Experiment

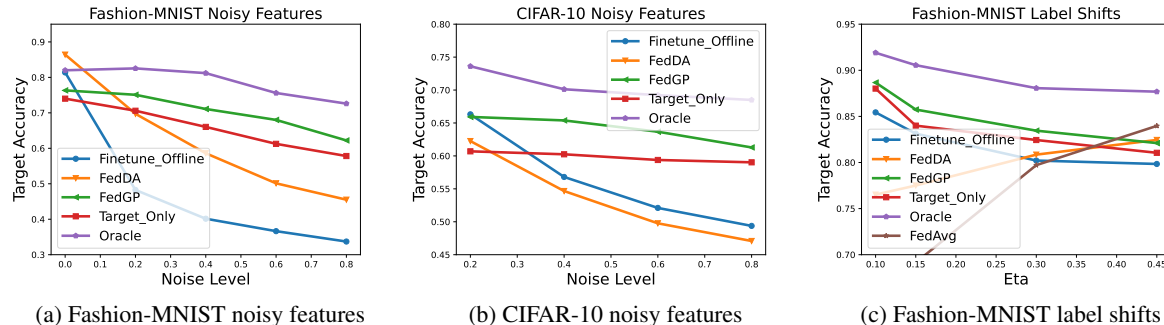


Figure 3: Under two settings (noisy features and label shifts), FedGP outperforms baselines in most cases and achieves a better bias-variance tradeoff. It also shows less sensitivity to the changing source-target shifts.

We empirically explore FedGP using a semi-synthetic experiment, where we manipulate the extent of domain shifts by adding different levels of Gaussian noise (noisy features) and degrees of class imbalance (label shifts). We show that the main impact comes from the shifts between target and source distributions.

Datasets and models. We create the semi-synthetic distribution shifts by adding different levels of feature noise and label shifts to Fashion-MNIST (Xiao et al., 2017) and CIFAR-10 (Krizhevsky et al., 2009) datasets, adapting from the Non-IID benchmark (Li et al., 2022). For models, we use a simple CNN model. Other details can be found in Appendix B.6. We set the communication round $R = 50$ and the local update epoch to 1, with 10 clients (1 target, 9 source clients) in the system.

Baselines. We compare the following methods: **FedAvg** (source only): we only use the source gradients by averaging. **Finetune_Offline**: we perform the same number of 50 epochs of fine-tuning after FedAvg. FedDA ($\beta = 0.5$): a convex combination with a middle trade-off point of source and target gradients. FedGP ($\beta = 0.5$): a middle trade-off point between source and target gradients with gradient projection. **Target Only**: we only use the target gradient ($\beta = 0$). **Oracle**: a fully-supervised training on the labeled target domain serving as the upper bound.

Setting 1: Noisy features. We add different levels of Gaussian noise to the target domain to control the source-target domain differences. For the Fashion-MNIST dataset, we add Gaussian noise levels of $std = (0.2, 0.4, 0.6, 0.8)$ to input images of the target client, in order to create various degrees of shifts between source and target domains. The task is to predict 10 classes on both source and target clients. For the CIFAR-10 dataset, we use the same noise levels, and the task is to predict 4 classes on both source and target clients. We use 100 labeled target samples for Fashion-MNIST, and 10% of the labeled target data for the CIFAR-10 dataset.

Setting 2: Label shifts. We split the Fashion-MNIST into two sets with 3 and 7 classes, respectively, denoted as D_1 and D_2 . A variable $\eta \in [0, 0.5]$ is used to control the difference between source and target clients by defining $D_S = \eta$ portion from D_1 and $(1 - \eta)$ portion from D_2 , $D_T = (1 - \eta)$ portion from D_1 and η portion from D_2 . When $\eta = 0.5$, there is no distribution shift, and when $\eta \rightarrow 0$, the shifts caused by label shifts become more severe. We use 15% labeled target samples for the target client. We test on cases with $\eta = [0.45, 0.30, 0.15, 0.10, 0.05, 0.00]$.

FedGP maintains a better trade-off between bias and variance. Figure 3 displays the performance trends of compared methods versus the change of source-target domain shifts. The full results are included in Table 6 and Table 7 in Appendix. In general, when the source-target domain difference grows bigger, FedDA, Finetune.Offline, and FedAvg degrade more severely compared with FedGP and Target Only, which trusts the target gradient more. We find that FedGP outperforms other baselines in most cases, showing a good ability to balance bias and variances under various conditions and being less sensitive to changing shifts. For the label shift cases, the target variance decreases as the domain shift grows bigger (easier to predict with fewer classes). Therefore, FedGP and Target Only surprisingly achieve higher performance with significant shift cases.

Connection with our theoretical insights. Interestingly, we see that when the shift is relatively small ($\eta = 0.45$ and 0 noise level for Fashion-MNIST), FedAvg and FedDA both outperform FedGP. Compared with what we have observed from our theory (Fig 2), adding increasing levels of noise can be regarded as going from left to right on the x-axis and when the shifts are small, we probably will get into an area where FedDA is better. When increasing the label shifts, we are increasing the shifts and decreasing the variances simultaneously, we go diagonally from the top-left to the lower-right in Figure 2, where we expect FedAvg is the best when we start from a small domain difference.

6.2 Real Dataset Experiments

Domains	ColoredMNIST			Avg	C	L	VLCS			Avg
	+90%	+80%	-90%				V	S		
FedAvg	56.82 (0.80)	62.37 (1.75)	27.77 (0.82)	48.99	90.49 (5.34)	60.65 (1.83)	70.24 (1.97)	69.10 (1.99)	72.62	
Finetune.Offline	66.58 (4.93)	69.09 (2.62)	53.86 (6.89)	63.18	96.65 (3.68)	68.22 (2.26)	74.34 (0.83)	74.66 (2.58)	78.47	
FedDA	60.49 (2.54)	65.07 (1.26)	33.04 (3.15)	52.87	97.72 (0.46)	68.17 (1.42)	75.27 (1.45)	76.68 (0.91)	79.46	
FedGP	88.14 (4.22)	76.34 (2.22)	89.80 (0.68)	84.76	99.43 (0.30)	71.09 (1.24)	73.65 (3.10)	78.70 (1.31)	80.72	
Target Only	85.60 (4.78)	73.54 (2.98)	87.05 (3.41)	82.06	97.77 (1.45)	68.88 (1.86)	72.29 (1.73)	76.00 (1.89)	78.74	
Oracle	89.94 (0.38)	80.32 (0.44)	89.99 (0.54)	86.75	100.00 (0.00)	72.72 (2.53)	78.65 (1.38)	82.71 (1.07)	83.52	

Table 1: **Target domain accuracy (%)** on ColoredMNIST and VLCS. FedGP outperforms the baselines in most cases and on average.

	TerraIncognita				
	L100	L38	L43	L46	Avg
FedAvg	54.62 (4.45)	31.39 (3.13)	36.85 (2.80)	27.15 (1.21)	37.50
Finetune.Offline	77.45 (3.88)	75.22 (5.46)	61.16 (4.07)	58.89 (7.95)	68.18
FedDA	77.24 (2.22)	69.21 (1.83)	58.55 (3.37)	53.78 (1.74)	64.70
FedGP	81.46 (1.28)	77.75 (1.55)	64.18 (2.86)	61.56 (1.94)	71.24
Target Only	78.85 (1.86)	74.25 (2.52)	58.96 (3.50)	56.90 (3.09)	67.24
Oracle	96.41 (0.18)	95.01 (0.28)	91.98 (1.17)	89.04 (0.93)	93.11

Table 2: **Target domain accuracy (%)** on TerraIncognita. FedGP outperforms the baselines in most cases and on average.

Datasets, models, and baselines. We use the Domainbed (Gulrajani & Lopez-Paz, 2020) benchmark with multiple domains, with realistic shifts between source and target clients. We conduct experiments on three datasets: ColoredMNIST (Arjovsky et al., 2019) (a dataset derived from MNIST (Deng, 2012) but with spurious features of colors), VLCS (Fang et al., 2013) (four datasets with five categories of bird, car, chair, dog, and person), and TerraIncognita (Beery et al., 2018) (consists of 57,868 images across 20 locations, each labeled with one of 15 classes) datasets. The task is to predict labels of the target domain by doing classification. We adapt mostly from the original benchmarks for the models: we use a CNN model for ColoredMNIST and ResNet-18 He et al. (2016) for the other two datasets. For baselines, we compare the same methods as in Section 6.1. Further comparison with the state-of-the-art (SOTA) unsupervised FDA method can be found in Appendix B.7.

Implementation. We set the communication round $R = 50$ and the local update epoch to 1. For each dataset, we test the target performance of individual domains using the left-out domain as the target and the rest as source domains. The accuracies are reported using 5 trials. Additionally, we use 0.1% labeled target samples for the ColoredMNIST dataset and 5% labeled samples for the rest two datasets.

FedGP is effective for real datasets. We report the individual and average FDA performance for each domain with the three datasets, as shown in Table 1 and Table 2. From the results, we observe that FedGP achieves the best performance in most cases with a comparatively large margin and an accuracy that is close to the upper bound. However, for the V domain in the VLCS case, FedDA is better than FedGP, we hypothesize that this is because the variance of the target gradient is relatively large in that case (Target Only is only slightly better than source only - FedAvg), leading to the situation where FedDA turns out to achieve a better bias-variance tradeoff. We find that offline fine-tuning works surprisingly well for the TerraIncognita dataset, with a performance close to FedGP, and it becomes worse than FedDA for the VLCS dataset. We think the initialization remains an important open question for the fine-tuning-based methods, which will be explored more in future work.

6.3 Ablation Study

The effect of target gradient variances. We conduct experiments with increasing numbers of labeled target samples (decreased target variances) with varying noise levels [0.2, 0.4, 0.6] on Fashion-MNIST with 10 clients in the system. We compare two aggregation rules FedGP and FedDA. When the number of labeled samples increases, the target performance also improves (the variance term becomes smaller). We discover that FedGP can predict quite well even with a small number of labeled samples, especially when the target gradient is very accurate (small variance), as in the Fashion-MNIST dataset.

	0.2		0.4		0.6	
	FedDA	FedGP	FedDA	FedGP	FedDA	FedGP
100	69.73	75.09	58.6	71.09	50.13	68.01
200	72.07	74.21	58.59	70.93	52.67	70.31
500	76.59	78.41	65.34	74.07	54.97	70.52
1000	77.92	78.68	68.26	75.17	59.16	71.63

Table 3: **Target domain accuracy (%)** by adding feature noise=0.2, 0.4, 0.6 on the Fashion-MNIST dataset with different numbers of labeled target samples.

The effect of bias-variance trade-off variable β . Figure 4 shows the results of experiments on the Fashion-MNIST dataset with a 0.4 noise level, along with testing β values of [0, 0.2, 0.4, 0.6, 0.8, 1.0]. For FedDA, we see it gets close to FedAvg when $\beta = 1$ and is the same as Target Only when $\beta = 0$. In contrast, with reference to an accurate target gradient, FedGP manages to perform well even when $\beta = 1.0$.

Effectiveness of projection and filtering. In Table 4, we illustrate the effectiveness of using gradient projection and filtering negative gradients in Fashion-MNIST noisy feature experiments. Compared with FedDA which does not perform gradient projection, FedGP manages to achieve a large margin (15%) of performance gain, especially when the shifts are larger. Further, with filtering, we generally get a 2% performance gain compared with no filtering.

6.4 Discussion

Initialization remains a challenging issue for fine-tuning methods. From both semi-synthetic and real-world experiments, we find an inconsistent pattern for the Offline_Finetuning method. It outperforms FedDA in some cases and is worse in others. We find an unclear effect of personalization – as it sometimes helps with adaptation

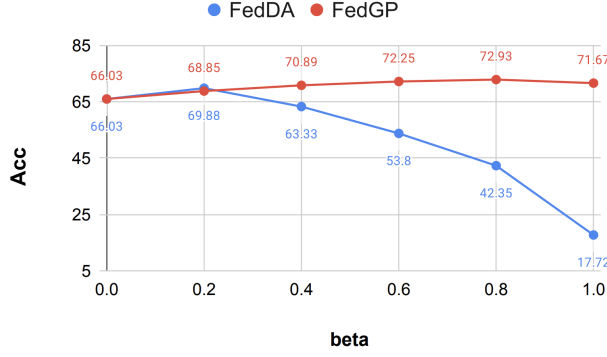


Figure 4: The effect of β on FedDA and FedGP.

Target noise level	0.2	0.4	0.6	0.8
FedDA(w/o projection)	69.73	58.6	50.13	45.51
FedGP(w/o filter)	72.93	69.51	65.46	60.70
FedGP(w filter)	75.09	71.09	68.01	62.22

Table 4: Effectiveness of the gradient projection and filtering for FedGP. FedGP is especially effective when the shifts are large.

performance or harms it. We leave further analysis to find the relationship between personalization and adaptation to future work. Further, the communication cost coming from offline fine-tuning is uncertain, i.e, how many iterations it requires to obtain a relatively good initialization.

Compared to the unsupervised state-of-the-art method (Feng et al., 2021) in Appendix B.7, we find FedGP has more stable performance across domains with better average performances. Though sometimes KD3A outperforms the FedGP and is fairly close to Oracle performances with comparatively small shift cases (VLCS dataset), in other cases, training on all unlabeled data seems to fail especially for the large shift cases (TerraIncognita dataset).

The computational complexity analysis of FedGP is discussed in Appendix B.3. In a real implementation, the whole process of projection is fast, with around 0.023 seconds per call needed for $N = 10$ clients of Fashion-MNIST experiments on the NVIDIA TITAN Xp hardware with GPU available.

7 Conclusion

We propose FedGP, a filtering-based aggregation rule for Federated Domain Adaptation via gradient projection. We provide a theoretical framework that first formally defines the metrics to connect FDA settings with aggregation rules. We investigate the well-rounded mechanism of FedGP theoretically and prove its effectiveness in comprehensive experiments. For future work, we would like to extend current metrics to real-world settings, explore the relationship between personalization and domain adaptation, and devise stronger aggregation rules for the FDA problem.

References

Arjovsky, M., Bottou, L., Gulrajani, I., and Lopez-Paz, D. Invariant risk minimization. *arXiv preprint arXiv:1907.02893*, 2019.

Beery, S., Van Horn, G., and Perona, P. Recognition in terra incognita. In *Proceedings of the European conference on computer vision (ECCV)*, pp. 456–473, 2018.

Cao, X., Fang, M., Liu, J., and Gong, N. Fltrust: Byzantine-robust federated learning via trust bootstrapping. In *Proceedings of NDSS*, 2021.

Deng, L. The mnist database of handwritten digit images for machine learning research. *IEEE Signal Processing Magazine*, 29(6):141–142, 2012.

Fang, C., Xu, Y., and Rockmore, D. N. Unbiased metric learning: On the utilization of multiple datasets and web images for softening bias. In *Proceedings of the IEEE International Conference on Computer Vision*, pp. 1657–1664, 2013.

Feng, H., You, Z., Chen, M., Zhang, T., Zhu, M., Wu, F., Wu, C., and Chen, W. Kd3a: Unsupervised multi-source decentralized domain adaptation via knowledge distillation. In Meila, M. and Zhang, T. (eds.), *Proceedings of the*

38th International Conference on Machine Learning, volume 139 of *Proceedings of Machine Learning Research*, pp. 3274–3283. PMLR, 18–24 Jul 2021.

Gulrajani, I. and Lopez-Paz, D. In search of lost domain generalization. In *International Conference on Learning Representations*, 2020.

He, C., Yang, Z., Mushtaq, E., Lee, S., Soltanolkotabi, M., and Avestimehr, S. Ssfl: Tackling label deficiency in federated learning via personalized self-supervision. *arXiv preprint arXiv:2110.02470*, 2021.

He, K., Zhang, X., Ren, S., and Sun, J. Deep residual learning for image recognition. In *Proceedings of the IEEE conference on computer vision and pattern recognition*, pp. 770–778, 2016.

Jeong, W., Yoon, J., Yang, E., and Hwang, S. J. Federated semi-supervised learning with inter-client consistency & disjoint learning. In *International Conference on Learning Representations*, 2020.

Karimireddy, S. P., Kale, S., Mohri, M., Reddi, S., Stich, S., and Suresh, A. T. SCAFFOLD: Stochastic controlled averaging for federated learning. In III, H. D. and Singh, A. (eds.), *Proceedings of the 37th International Conference on Machine Learning*, volume 119 of *Proceedings of Machine Learning Research*, pp. 5132–5143. PMLR, 13–18 Jul 2020.

Kingma, D. P. and Ba, J. Adam: A method for stochastic optimization. *arXiv preprint arXiv:1412.6980*, 2014.

Krizhevsky, A., Hinton, G., et al. Learning multiple layers of features from tiny images. 2009.

Li, Q., Diao, Y., Chen, Q., and He, B. Federated learning on non-iid data silos: An experimental study. In *IEEE International Conference on Data Engineering*, 2022.

Li, X., Gu, Y., Dvornek, N., Staib, L. H., Ventola, P., and Duncan, J. S. Multi-site fmri analysis using privacy-preserving federated learning and domain adaptation: Abide results. *Medical Image Analysis*, 65:101765, 2020.

Liang, J., Hu, D., and Feng, J. Do we really need to access the source data? Source hypothesis transfer for unsupervised domain adaptation. In III, H. D. and Singh, A. (eds.), *Proceedings of the 37th International Conference on Machine Learning*, volume 119 of *Proceedings of Machine Learning Research*, pp. 6028–6039. PMLR, 13–18 Jul 2020.

McMahan, B., Moore, E., Ramage, D., Hampson, S., and Arcas, B. A. y. Communication-Efficient Learning of Deep Networks from Decentralized Data. In Singh, A. and Zhu, J. (eds.), *Proceedings of the 20th International Conference on Artificial Intelligence and Statistics*, volume 54 of *Proceedings of Machine Learning Research*, pp. 1273–1282. PMLR, 20–22 Apr 2017.

Nguyen, T., Le, T., Zhao, H., Tran, Q. H., Nguyen, T., and Phung, D. Most: Multi-source domain adaptation via optimal transport for student-teacher learning. In *Uncertainty in Artificial Intelligence*, pp. 225–235. PMLR, 2021.

Peng, X., Huang, Z., Zhu, Y., and Saenko, K. Federated adversarial domain adaptation. In *International Conference on Learning Representations*, 2020.

Saito, K., Watanabe, K., Ushiku, Y., and Harada, T. Maximum classifier discrepancy for unsupervised domain adaptation. In *Proceedings of the IEEE conference on computer vision and pattern recognition*, pp. 3723–3732, 2018.

Wang, H., Yurochkin, M., Sun, Y., Papailiopoulos, D., and Khazaeni, Y. Federated learning with matched averaging. In *International Conference on Learning Representations*, 2019.

Wu, G. and Gong, S. Collaborative optimization and aggregation for decentralized domain generalization and adaptation. In *Proceedings of the IEEE/CVF International Conference on Computer Vision (ICCV)*, pp. 6484–6493, October 2021.

Xiao, H., Rasul, K., and Vollgraf, R. Fashion-mnist: a novel image dataset for benchmarking machine learning algorithms. *arXiv preprint arXiv:1708.07747*, 2017.

Xie, C., Koyejo, S., and Gupta, I. Zeno++: Robust fully asynchronous SGD. In III, H. D. and Singh, A. (eds.), *Proceedings of the 37th International Conference on Machine Learning*, volume 119 of *Proceedings of Machine Learning Research*, pp. 10495–10503. PMLR, 13–18 Jul 2020a.

Xie, M., Long, G., Shen, T., Zhou, T., Wang, X., Jiang, J., and Zhang, C. Multi-center federated learning, 2020b.

Yang, D., Xu, Z., Li, W., Myronenko, A., Roth, H. R., Harmon, S., Xu, S., Turkbey, B., Turkbey, E., Wang, X., et al. Federated semi-supervised learning for covid region segmentation in chest ct using multi-national data from china, italy, japan. *Medical image analysis*, 70:101992, 2021.

Zhao, H., Zhang, S., Wu, G., Moura, J. M., Costeira, J. P., and Gordon, G. J. Adversarial multiple source domain adaptation. *Advances in neural information processing systems*, 31, 2018.

A Proofs

Theorem A.1 (Theorem 4.4 Restated). *Consider model parameter $\theta \sim \pi$ and an aggregation rule $\text{Aggr}(\cdot)$ with step size $\mu > 0$. Define the updated parameter as*

$$\theta^+ := \theta - \mu \hat{g}_{\text{Aggr}}(\theta).$$

Assuming the gradient $\nabla \ell(\theta, z)$ is γ -Lipschitz in θ for any z , and let the step size $\mu = \frac{1}{\gamma}$, we have

$$\mathbb{E}_{\widehat{\mathcal{D}}_T, \theta} [\ell_{\mathcal{D}_T}(\theta^+) - \ell_{\mathcal{D}_T}(\theta)] \leq -\frac{1}{2\gamma} (\|g_{\mathcal{D}_T}\|_\pi^2 - \Delta_{\text{Aggr}}^2).$$

Proof. Given any distribution data \mathcal{D} , we first prove that $\nabla \ell_{\mathcal{D}}$ is also γ -Lipschitz as below. For $\forall \theta_1, \theta_2 \in \Theta$:

$$\begin{aligned} \|\nabla \ell_{\mathcal{D}}(\theta_1) - \nabla \ell_{\mathcal{D}}(\theta_2)\| &= \|\mathbb{E}_{z \sim \mathcal{D}} [\nabla \ell(\theta_1, z) - \nabla \ell(\theta_2, z)]\| \\ &\leq \mathbb{E}_{z \sim \mathcal{D}} \|\nabla \ell(\theta_1, z) - \nabla \ell(\theta_2, z)\| \quad (\text{Jensen's inequality}) \\ &\leq \mathbb{E}_{z \sim \mathcal{D}} \gamma \|\theta_1 - \theta_2\| \quad (\nabla \ell(\cdot, z) \text{ is } \gamma\text{-Lipschitz}) \\ &= \gamma \|\theta_1 - \theta_2\|. \end{aligned}$$

Therefore, we know that $\ell_{\mathcal{D}_T}$ is γ -smooth. Conditioned on a θ and a $\widehat{\mathcal{D}}_T$, and apply the definition of smoothness we have

$$\begin{aligned} \ell_{\mathcal{D}_T}(\theta^+) - \ell_{\mathcal{D}_T}(\theta) &\leq \langle \nabla \ell_{\mathcal{D}_T}(\theta), \theta^+ - \theta \rangle + \frac{\gamma}{2} \|\theta^+ - \theta\|^2 \\ &= -\langle \nabla \ell_{\mathcal{D}_T}(\theta), \mu \hat{g}_{\text{Aggr}}(\theta) \rangle + \frac{\gamma}{2} \|\mu \hat{g}_{\text{Aggr}}(\theta)\|^2 \\ &= -\mu \langle \nabla \ell_{\mathcal{D}_T}(\theta), \hat{g}_{\text{Aggr}}(\theta) - \nabla \ell_{\mathcal{D}_T}(\theta) + \nabla \ell_{\mathcal{D}_T}(\theta) \rangle + \frac{\gamma \mu^2}{2} \|\hat{g}_{\text{Aggr}}(\theta) - \nabla \ell_{\mathcal{D}_T}(\theta) + \nabla \ell_{\mathcal{D}_T}(\theta)\|^2 \\ &= -\mu (\langle \nabla \ell_{\mathcal{D}_T}(\theta), \hat{g}_{\text{Aggr}}(\theta) - \nabla \ell_{\mathcal{D}_T}(\theta) \rangle + \|\nabla \ell_{\mathcal{D}_T}(\theta)\|^2) \\ &\quad + \frac{\gamma \mu^2}{2} (\|\hat{g}_{\text{Aggr}}(\theta) - \nabla \ell_{\mathcal{D}_T}(\theta)\|^2 + \|\nabla \ell_{\mathcal{D}_T}(\theta)\|^2 + 2 \langle \hat{g}_{\text{Aggr}}(\theta) - \nabla \ell_{\mathcal{D}_T}(\theta), \nabla \ell_{\mathcal{D}_T}(\theta) \rangle). \end{aligned}$$

Applying that $\mu = \frac{1}{\gamma}$ we can derive from the above that

$$\begin{aligned} \ell_{\mathcal{D}_T}(\theta^+) - \ell_{\mathcal{D}_T}(\theta) &\leq \frac{1}{2\gamma} (\|\hat{g}_{\text{Aggr}}(\theta) - \nabla \ell_{\mathcal{D}_T}(\theta)\|^2 - \|\nabla \ell_{\mathcal{D}_T}(\theta)\|^2) \\ &= -\frac{1}{2\gamma} (\|\nabla \ell_{\mathcal{D}_T}(\theta)\|^2 - \|\hat{g}_{\text{Aggr}}(\theta) - \nabla \ell_{\mathcal{D}_T}(\theta)\|^2). \end{aligned}$$

Note that we denote $g_{\mathcal{D}_T} = \nabla \ell_{\mathcal{D}_T}$. Taking the expectation $\mathbb{E}_{\widehat{\mathcal{D}}_T, \theta}$ on both sides gives the theorem. \square

Theorem A.2 (Theorem 4.5 Restated).

$$\Delta_{\text{FedDA}}^2 = (1 - \beta)^2 \sigma_\pi^2(\widehat{\mathcal{D}}_T) + \beta^2 d_\pi^2(\mathcal{D}_S, \mathcal{D}_T).$$

Proof. Recall that

$$\hat{g}_{\text{FedDA}} = (1 - \beta)g_{\widehat{\mathcal{D}}_T} + \frac{\beta}{N} \sum_{i=1}^N g_{\mathcal{D}_{S_i}} = (1 - \beta)g_{\widehat{\mathcal{D}}_T} + \beta g_{\mathcal{D}_S}.$$

Plugging this into the definition of Δ_{FedDA}^2 , we have

$$\begin{aligned} \Delta_{\text{FedDA}}^2 &= \mathbb{E}_{\widehat{\mathcal{D}}_T} \|g_{\mathcal{D}_T} - \hat{g}_{\text{FedDA}}\|_\pi^2 = \mathbb{E}_{\widehat{\mathcal{D}}_T} \|g_{\mathcal{D}_T} - (1 - \beta)g_{\widehat{\mathcal{D}}_T} - \beta g_{\mathcal{D}_S}\|_\pi^2 \\ &= \mathbb{E}_{\widehat{\mathcal{D}}_T} \|(1 - \beta)(g_{\mathcal{D}_T} - g_{\widehat{\mathcal{D}}_T}) + \beta(g_{\mathcal{D}_T} - g_{\mathcal{D}_S})\|_\pi^2 \\ &= (1 - \beta)^2 \mathbb{E}_{\widehat{\mathcal{D}}_T} \|g_{\mathcal{D}_T} - g_{\widehat{\mathcal{D}}_T}\|_\pi^2 + \beta^2 \|g_{\mathcal{D}_T} - g_{\mathcal{D}_S}\|_\pi^2 + 2(1 - \beta)\beta \mathbb{E}_{\widehat{\mathcal{D}}_T} \langle g_{\mathcal{D}_T} - g_{\widehat{\mathcal{D}}_T}, g_{\mathcal{D}_T} - g_{\mathcal{D}_S} \rangle_\pi \\ &= (1 - \beta)^2 \sigma_\pi^2(\widehat{\mathcal{D}}_T) + \beta^2 d_\pi^2(\mathcal{D}_S, \mathcal{D}_T) + 2(1 - \beta)\beta \langle \mathbb{E}_{\widehat{\mathcal{D}}_T} [g_{\mathcal{D}_T} - g_{\widehat{\mathcal{D}}_T}], g_{\mathcal{D}_T} - g_{\mathcal{D}_S} \rangle_\pi \\ &= (1 - \beta)^2 \sigma_\pi^2(\widehat{\mathcal{D}}_T) + \beta^2 d_\pi^2(\mathcal{D}_S, \mathcal{D}_T). \end{aligned}$$

\square

Theorem A.3 (Theorem 4.6 Restated). *Consider FedGP in the setting where there is only one source client. We have*

$$\begin{aligned}\Delta_{\text{FedGP}}^2 &= (1 - \beta)^2 \sigma_\pi^2(\widehat{\mathcal{D}}_T) + \beta^2 E_{\theta, \widehat{\mathcal{D}}_T} [\widehat{\delta}(\theta) \tau^2(\theta) \|g_{\mathcal{D}_T}(\theta) - g_{\mathcal{D}_S}(\theta)\|^2] \\ &\quad + (2\beta - \beta^2) \mathbb{E}_{\theta, \widehat{\mathcal{D}}_T} \widehat{\delta}(\theta) \langle g_{\widehat{\mathcal{D}}_T}(\theta) - g_{\mathcal{D}_T}(\theta), u_{\mathcal{D}_S}(\theta) \rangle^2 \\ &\quad + 2(1 - \beta)\beta \mathbb{E}_{\theta, \widehat{\mathcal{D}}_T} [\widehat{\delta}(\theta) \langle g_{\mathcal{D}_T}(\theta), g_{\mathcal{D}_S}(\theta) \rangle \langle g_{\widehat{\mathcal{D}}_T}(\theta) - g_{\mathcal{D}_T}(\theta), u_{\mathcal{D}_S}(\theta) \rangle] + \beta^2 \mathbb{E}_{\theta, \widehat{\mathcal{D}}_T} [(1 - \widehat{\delta}(\theta)) \|g_{\mathcal{D}_T}(\theta)\|^2]\end{aligned}$$

In the above equation, $\widehat{\delta}(\theta) := \mathbf{1}(\langle g_{\widehat{\mathcal{D}}_T}(\theta), g_{\mathcal{D}_S}(\theta) \rangle > 0)$ is the indicator function and it is 1 if the condition is satisfied. $\tau(\theta) = \frac{\|g_{\mathcal{D}_T}(\theta) \sin \rho(\theta)\|}{\|g_{\mathcal{D}_S}(\theta) - g_{\mathcal{D}_T}(\theta)\|}$ where $\rho(\theta)$ is the angle between $g_{\mathcal{D}_S}(\theta)$ and $g_{\mathcal{D}_T}(\theta)$. Moreover, $u_{\mathcal{D}_S}(\theta) = g_{\mathcal{D}_S}(\theta) / \|g_{\mathcal{D}_S}(\theta)\|$.

Proof. Recall that

$$\Delta_{\text{FedGP}}^2 = \mathbb{E}_{\widehat{\mathcal{D}}_T} \|g_{\mathcal{D}_T} - \widehat{g}_{\text{FedGP}}\|_\pi^2 = \mathbb{E}_{\widehat{\mathcal{D}}_T, \theta} \|g_{\mathcal{D}_T}(\theta) - \widehat{g}_{\text{FedGP}}(\theta)\|^2.$$

Recall the definition of $\widehat{g}_{\text{FedGP}}$ is that

$$\begin{aligned}\widehat{g}_{\text{FedGP}}(\theta) &= (1 - \beta)g_{\widehat{\mathcal{D}}_T}(\theta) + \beta \max\{\langle g_{\widehat{\mathcal{D}}_T}(\theta), g_{\mathcal{D}_S} \rangle, 0\} g_{\mathcal{D}_S}(\theta) / \|g_{\mathcal{D}_S}(\theta)\|^2 \\ &= (1 - \beta)g_{\widehat{\mathcal{D}}_T}(\theta) + \beta \widehat{\delta}(\theta) \langle g_{\widehat{\mathcal{D}}_T}(\theta), u_{\mathcal{D}_S}(\theta) \rangle u_{\mathcal{D}_S}(\theta).\end{aligned}$$

Let us fix θ and then further simplify the notation by denoting

$$\begin{aligned}\hat{v} &:= g_{\widehat{\mathcal{D}}_T}(\theta) \\ v &:= g_{\mathcal{D}_T}(\theta) \\ u &:= u_{\mathcal{D}_S}(\theta) \\ \hat{\delta} &:= \hat{\delta}(\theta)\end{aligned}$$

Therefore, we have $\widehat{g}_{\text{FedGP}}(\theta) = (1 - \beta)\hat{v} + \beta\hat{\delta}\langle\hat{v}, u\rangle u$.

Therefore, with the simplified notation,

$$\begin{aligned}\mathbb{E}_{\widehat{\mathcal{D}}_T} \|g_{\mathcal{D}_T} - \widehat{g}_{\text{FedGP}}(\theta)\|^2 &= \mathbb{E}_{\widehat{\mathcal{D}}_T} \|(1 - \beta)\hat{v} + \beta\hat{\delta}\langle\hat{v}, u\rangle u - v\|^2 \\ &= \mathbb{E}_{\widehat{\mathcal{D}}_T} \|\beta(\hat{\delta}\langle\hat{v}, u\rangle u - v) + (1 - \beta)(\hat{v} - v)\|^2 \\ &= \mathbb{E}_{\widehat{\mathcal{D}}_T} \|\beta\hat{\delta}\langle\hat{v} - v, u\rangle u + \beta(\hat{\delta}\langle v, u\rangle u - v) + (1 - \beta)(\hat{v} - v)\|^2 \\ &= \beta^2 \mathbb{E}_{\widehat{\mathcal{D}}_T} [\hat{\delta}\langle\hat{v} - v, u\rangle^2] + \beta^2 \mathbb{E}_{\widehat{\mathcal{D}}_T} [\|\hat{\delta}\langle v, u\rangle u - v\|^2] + (1 - \beta)^2 \mathbb{E}_{\widehat{\mathcal{D}}_T} [\|\hat{v} - v\|^2] \\ &\quad + 2\beta(1 - \beta) \mathbb{E}_{\widehat{\mathcal{D}}_T} [\hat{\delta}\langle\hat{v} - v, u\rangle^2] + 2\beta(1 - \beta) \mathbb{E}_{\widehat{\mathcal{D}}_T} [\hat{\delta}\langle v, u\rangle \langle u, \hat{v} - v \rangle] \\ &\quad - 2\beta^2 \mathbb{E}[\hat{\delta}(1 - \hat{\delta})\langle\hat{v} - v, u\rangle \langle v, u \rangle] \quad (\text{expanding the squared norm}) \\ &= (2\beta - \beta^2) \mathbb{E}_{\widehat{\mathcal{D}}_T} [\hat{\delta}\langle\hat{v} - v, u\rangle^2] + \beta^2 \underbrace{\mathbb{E}_{\widehat{\mathcal{D}}_T} [\|\hat{\delta}\langle v, u\rangle u - v\|^2]}_A + (1 - \beta)^2 \mathbb{E}_{\widehat{\mathcal{D}}_T} [\|\hat{v} - v\|^2] \\ &\quad + 2\beta(1 - \beta) \mathbb{E}_{\widehat{\mathcal{D}}_T} [\hat{\delta}\langle v, u\rangle \langle u, \hat{v} - v \rangle] - 2\beta^2 \underbrace{\mathbb{E}[\hat{\delta}(1 - \hat{\delta})\langle\hat{v} - v, u\rangle \langle v, u \rangle]}_B,\end{aligned}$$

where the last equality is by merging the similar terms. Next, we deal with the terms A and B .

Let us start from the term B . Noting that $\hat{\delta}$ is either 0 or 1, we can see that $\hat{\delta}(1 - \hat{\delta}) = 0$. Therefore, $B = 0$.

As for the term A , noting that $\hat{\delta}^2 = \hat{\delta}$, expanding the squared term we have:

$$\begin{aligned}A &= \mathbb{E}_{\widehat{\mathcal{D}}_T} [\|\hat{\delta}\langle v, u\rangle u - v\|^2] = \mathbb{E}_{\widehat{\mathcal{D}}_T} [\|\hat{\delta}(\langle v, u\rangle u - v) - (1 - \hat{\delta})v\|^2] \\ &= \mathbb{E}_{\widehat{\mathcal{D}}_T} [\hat{\delta}\|\langle v, u\rangle u - v\|^2] + \mathbb{E}_{\widehat{\mathcal{D}}_T} [(1 - \hat{\delta})\|v\|^2] - 2\mathbb{E}_{\widehat{\mathcal{D}}_T} [\hat{\delta}(1 - \hat{\delta})\langle\langle v, u\rangle u - v, v \rangle] \\ &= \mathbb{E}_{\widehat{\mathcal{D}}_T} [\hat{\delta}\|\langle v, u\rangle u - v\|^2] + \mathbb{E}_{\widehat{\mathcal{D}}_T} [(1 - \hat{\delta})\|v\|^2].\end{aligned}$$

Algorithm 1 Federated Domain Adaptation

Input: N source domains $\mathcal{D}_S = \{\mathcal{D}_{S_i}\}_{i=1}^N$, target domain \mathcal{D}_T ; N source clients $\{\mathcal{C}_{S_i}\}_{i=1}^N$, target client \mathcal{C}_T , server \mathcal{S} ; number of rounds R ; aggregation rule aggr ; variance-bias trade-off parameter β .

Initialize $h_{S_1}^{(0)}, h_{S_2}^{(0)}, \dots, h_{S_N}^{(0)}$ and $h_T^{(0)}$.

for $r = 1, 2, \dots, R$ **do**

- for** \mathcal{C}_{S_i} in $\{\mathcal{C}_{S_i}\}_{i=1}^N$ **do**
- Initialize $h_{S_i}^{(r)} \leftarrow h_{global}^{(r-1)}$
- Optimize $h_{S_i}^{(r)}$ on \mathcal{D}_{S_i}
- Send $h_{S_i}^{(r)}$ to \mathcal{S}
- end for**
- for** h_{S_i} in $\{h_{S_i}^{(r)}\}_{i=1}^N$ **do**
- \mathcal{S} computes $g_i \leftarrow h_{S_i}^{(r)} - h_{global}^{(r-1)}$
- end for**
- \mathcal{S} sends $\{g_i\}_{i=1}^N$ to \mathcal{C}_T
- \mathcal{C}_T initializes $h_T^{(r)} \leftarrow h_{global}^{(r-1)}$
- \mathcal{C}_T optimizes $h_T^{(r)}$ on \mathcal{D}_T using labeled samples
- \mathcal{C}_T computes $g_T \leftarrow h_T^{(r)} - h_{global}^{(r-1)}$
- \mathcal{C}_T updates the global model as
- $h_{global}^{(r)} \leftarrow h_{global}^{(r-1)} + \text{aggr}(\{g_i\}_{i=1}^N, g_T, \beta)$
- \mathcal{C}_T sends $h_{global}^{(r)}$ to \mathcal{S}
- \mathcal{S} broadcasts $h_{global}^{(r)}$ to $\{\mathcal{C}_{S_i}\}_{i=1}^N$

end for

Therefore, combining the above, we have

$$\begin{aligned} \mathbb{E}_{\widehat{\mathcal{D}}_T} \|g_{\mathcal{D}_T}(\theta) - \widehat{g}_{\text{FedGP}}(\theta)\|^2 &= (1 - \beta)^2 \mathbb{E}_{\widehat{\mathcal{D}}_T} [\|\hat{v} - v\|^2] + \beta^2 \mathbb{E}_{\widehat{\mathcal{D}}_T} [\hat{\delta} \|\langle v, u \rangle u - v\|^2] + (2\beta - \beta^2) \mathbb{E}_{\widehat{\mathcal{D}}_T} [\hat{\delta} \langle \hat{v} - v, u \rangle^2] \\ &\quad + 2\beta(1 - \beta) \mathbb{E}_{\widehat{\mathcal{D}}_T} [\hat{\delta} \langle v, u \rangle \langle u, \hat{v} - v \rangle] + \beta^2 \mathbb{E}_{\widehat{\mathcal{D}}_T} [(1 - \hat{\delta}) \|v\|^2]. \end{aligned}$$

Let us give an alternative form for $\|\langle v, u \rangle u - v\|^2$, as we aim to connect this term to $\|u - v\|$ which would become the domain-shift. Note that $\|\langle v, u \rangle u - v\|$ is the distance between v and its projection to u . We can see that $\|\langle v, u \rangle u - v\| = \|u - v\| \frac{\|\langle v, u \rangle u - v\|}{\|u - v\|} = \|u - v\| \tau(\theta)$. Therefore, pluggin this in, we have

$$\begin{aligned} \mathbb{E}_{\widehat{\mathcal{D}}_T} \|g_{\mathcal{D}_T}(\theta) - \widehat{g}_{\text{FedGP}}(\theta)\|^2 &= (1 - \beta)^2 \mathbb{E}_{\widehat{\mathcal{D}}_T} [\|\hat{v} - v\|^2] + \beta^2 \mathbb{E}_{\widehat{\mathcal{D}}_T} [\hat{\delta} \|u - v\|^2 \tau^2(\theta)] + (2\beta - \beta^2) \mathbb{E}_{\widehat{\mathcal{D}}_T} [\hat{\delta} \langle \hat{v} - v, u \rangle^2] \\ &\quad + 2\beta(1 - \beta) \mathbb{E}_{\widehat{\mathcal{D}}_T} [\hat{\delta} \langle v, u \rangle \langle u, \hat{v} - v \rangle] + \beta^2 \mathbb{E}_{\widehat{\mathcal{D}}_T} [(1 - \hat{\delta}) \|v\|^2] \end{aligned}$$

Writing the abbreviations $u, v, \hat{v}, \hat{\delta}$ into their original forms and taking expectation over θ on the both side we can derive the theorem. □

B Additional Experiment Information

B.1 Algorithm outlines for Federated Domain Adaptation

As illustrated in Algorithm 1, for one communication round, each source client \mathcal{C}_{S_i} performs supervised training on its own data distribution \mathcal{D}_{S_i} and uploads the weights to the server. Then the server computes and shuffles the source gradients, sending them to the target client \mathcal{C}_T . On \mathcal{C}_T , it updates its parameter using the labeled target data. After that, the target client updates the global model using proposed aggregation rules (FedDA, FedGP) and sends the model to the server. The server then broadcasts the new weight to all source clients, which completes one round.

B.2 Implementation Details of GP

We compute the model updates from source and target clients as $G_{S_i}^{(r)} \simeq h_{S_i}^{(r)} - h_{global}^{(r-1)}$ and $G_T^{(r)} \simeq h_T^{(r)} - h_T^{(r-1)}$, respectively. In our real training process, because we use different learning rates, and training samples for source and target clients, we need to **align the magnitude of model updates**. We first align the model updates from source clients to the target client and combine the projection results with the target updates. We use lr_T and lr_S to denote the target and source learning rates; $batchsize_T$ and $batchsize_S$ are the batch sizes for target and source domains, respectively; n_l is the labeled sample size on target client and n_i is the sample size for source client C_{S_i} ; r_S is the rounds of local updates on source clients. The total gradient projection P_{GP} from all source clients $\{G_{S_i}^{(r)}\}_{i=1}^N$ projected on the target direction G_T could be computed as Eq. B.2. We use \mathcal{L} to denote all layers of current model updates. n_i denotes the number of samples trained on source client C_{S_i} , which is adapted from FedAvg (McMahan et al., 2017) to redeem data imbalance issue. Hence, we normalize the gradient projections according to the number of samples. Also, $+\sum_{l \in \mathcal{L}}$ concatenates the projected gradients of all layers.

$$P_{GP} = \sum_{i=0}^N \left(\mathbf{GP} \left(\left(h_{S_i}^{(r)} - h_{global}^{(r-1)} \right)^l, \left(h_T^{(r)} - h_T^{(r-1)} \right)^l \right) \cdot \frac{n_i}{\sum_i^N n_i} \cdot \frac{\frac{n_l}{batchsize_T}}{\frac{n_i}{batchsize_S}} \cdot \frac{lr_T}{lr_S} \cdot \frac{1}{r_S} \cdot \left(h_{S_i}^{(r)} - h_{global}^{(r-1)} \right) \right)$$

Lastly, a hyper-parameter β is used to incorporate target update G_T into P_{GP} to have a more stable performance. The final target model weight $h_T^{(r)}$ at round r is thus expressed as:

$$h_T^{(r)} = h_T^{(r-1)} + (1 - \beta) \cdot P_{GP} + \beta \cdot G_T$$

B.3 Derivation of Gradient Projection Method's Time and Space Complexity

Time complexity: Assume the total parameter is m and we have l layers. To make it simpler, assume each layer has an average of $\frac{m}{l}$ parameters. Computing cosine similarity for all layers of one source client is $O\left(\left(\frac{m}{l}\right)^2 \cdot l\right) = O(m^2/l)$. We have N source clients so the total time cost for GP is $O(N \cdot m^2/l)$.

Space complexity: The extra memory cost for GP (computing cosine similarity) is $O(1)$ per client for storing the current cosine similarity value.

B.4 Impact of Extent of Shifts Between Source Clients

In addition to the source-target domain differences, we also experiment with different degrees of shifts within source clients. To control the extent of shifts between source clients, we use a target noise = 0.4 with [3, 5, 7, 9] labels available. From the results, we discover the shifts between source clients themselves have less impact on the target domain performance. For example, the 3-label case (a bigger shift) generally outperforms the 5-label one with a smaller shift. Therefore, we argue that the source-target shift serves as the main factor for an evident performance pattern.

Number of labels	9	7	3	5
FedAvg	11.27	18.81	25.54	34.11
Finetune_Offline	37.79	64.75	68.69	65.41
FedDA_0.5	55.01	57.9	54.16	61.62
FedGP_0.5	68.50	68.64	64.43	66.59
FedGP_1	65.27	59.07	26.37	39.86
Target_Only	63.06	65.76	61.8	63.65
Oracle	81.2	81.2	81.2	81.2

Table 5: **Target domain accuracy (%)** on label shifts with [3,5,7,9] labels available on Fashion-MNIST dataset with target noise = 0.4 and 100 target labeled samples.

Target noise	Fashion-MNIST				CIFAR-10				
	0	0.2	0.4	0.6	0.8	0.2	0.4	0.6	0.8
FedAvg	83.94	25.49	18.55	16.71	14.99	20.48	17.61	16.44	16.27
Finetune_Offline	81.39	48.26	40.15	36.64	33.71	66.31	56.80	52.10	49.37
FedDA_0.5	86.41	69.73	58.6	50.13	45.51	62.25	54.67	49.77	47.08
FedGP_0.5	76.33	75.09	71.09	68.01	62.22	66.40	65.28	63.29	61.59
FedGP_1	79.40	77.03	71.67	63.71	54.18	21.46	20.75	19.31	18.26
Target Only	74.00	70.59	66.03	61.26	57.82	60.69	60.25	59.38	59.03
Oracle	82.00	82.53	81.20	75.60	72.60	73.61	70.12	69.22	68.50

Table 6: **Target domain accuracy (%)** by adding feature noise to Fashion-MNIST and CIFAR-10 datasets using different aggregation rules.

η	0.45	0.3	0.15	0.1	0.05	0
FedAvg	83.97	79.71	69.15	59.90	52.51	0.00
Finetune_Offline	79.84	80.21	83.13	85.43	89.63	33.25
FedDA_0.5	82.44	80.85	77.50	76.51	68.26	59.56
FedGP_0.5	82.97	83.24	85.97	88.72	91.89	98.71
FedGP_1	77.41	73.12	62.54	53.56	27.62	0.00
Target only	81.05	82.44	84.00	88.02	89.80	98.32
Oracle	87.68	88.06	90.56	91.9	93.46	98.73

Table 7: **Target domain accuracy (%)** by adding feature noise to the Fashion-MNIST dataset using different aggregation rules.

B.5 Full Results on Noisy Features and Label Shifts Experiments on Non-IID Datasets

B.6 Implementation Details

NonIID Experiments. For the experiments on the Fashion-MNIST dataset, we set the source learning rate to be 0.01 and the target learning rate to 0.05. For CIFAR-10, we use a 0.005 source learning rate and a 0.0025 learning rate. The source batch size is set to 64 and the target batch size is 16. We partition the data to clients using the same procedure described in the benchmark (Li et al., 2022). For the model, we use a CNN model architecture consisting of two convolutional layers and three fully-connected layers. We use cross-entropy loss as the criterion and apply the Adam (Kingma & Ba, 2014) optimizer. **Domainbed Experiments.** The source learning rate is set to $1e^{-3}$ for ColoredMNIST and $5e^{-5}$ for VLCS and TerraIncognita. The target learning rate is set to $\frac{1}{5}$ of the source learning rate. For source domains, we split the training/testing data with a 20% and 80% split. For the target domain, we use a fraction (0.1% for Colored-MNIST, 5% for VLCS, and TerraIncognita) of the 80% split of training data to compute the target gradient and report the target accuracy on the test split of the data. For Colored-MNIST, we use a CNN model with four convolutional and batch-norm layers. We use the cross-entropy loss as the criterion and apply the Adam (Kingma & Ba, 2014) optimizer.

B.7 Comparison with the Unsupervised SOTA Method

	VLCS				TerraIncognita					
	C	L	V	S	Avg	L100	L38	L43	L46	Avg
KD3A (Feng et al., 2021)	99.64	63.28	78.07	80.49	79.01	62.24	37.19	28.09	28.4	38.98
FedGP	99.43	71.09	73.65	78.70	80.72	81.46	77.75	64.18	61.56	71.24
Oracle	100.00	72.72	78.65	82.71	83.52	96.41	95.01	91.98	89.04	93.11

Table 8: Performance comparison with the unsupervised SOTA method.